Wall Stabilized Operation in High Beta NSTX Plasmas

S.A. Sabbagh 1), A.C. Sontag 1), J.M. Bialek 1), D.A. Gates 2), A.H. Glasser 3), J.E. Menard 2), W. Zhu 1), M.G. Bell 2), R.E. Bell 2), A. Bondeson 4), C.E. Bush 5), J.D. Callen 6), M.S. Chu 7), S.M. Kaye 2), L.L. Lao 7), B.P. LeBlanc 2), Y. Liu 4), R. Maingi 5), D. Mueller 2), K.C. Shaing 6), D. Stutman 8), K. Tritz 8), C. Zhang 9)

1) Department of Applied Physics and Applied Mathematics, Columbia University, New York, NY, USA
2) Princeton Plasma Physics Laboratory, Princeton University, Princeton, NJ, USA
3) Los Alamos National Laboratory, Los Alamos, NM, USA
4) Institute for Electromagnetic Field Theory, Chalmers U., Goteborg, Sweden
5) Oak Ridge National Laboratory, Oak Ridge, TN, USA
6) University of Wisconsin, Madison, WI, USA
7) General Atomics, San Diego, CA, USA
8) Johns Hopkins University, Baltimore, MD, USA
9) Institute of Plasma Physics, Chinese Academy of Sciences, Hefei, China

e-mail contact of main author: sabbagh@pppl.gov

Abstract. The National Spherical Torus Experiment, NSTX, has demonstrated the advantages of low aspect ratio geometry in accessing high $\beta_t \equiv 2\mu_0\langle p\rangle/B_0^2$ and $\beta_N \equiv 10^8\langle\beta_t\rangle aB_0/I_p$. Experiments have reached β_t = 39% through boundary and profile optimization and β_N = 6.8 utilizing moderate current profile modification. High β_N plasmas can exceed the ideal no-wall stability limit, $\beta_{Nno\text{-}wall}$, for periods much greater than the wall eddy current decay time. Resistive wall mode (RWM) physics is studied to understand mode stabilization in these plasmas. The toroidal mode spectrum of unstable RWMs has been measured with mode number n up to 3. The critical rotation frequency of Bondeson-Chu, $\Omega_{crit} = \omega_A/(4q^2)$ describes well the RWM stability of NSTX plasmas when applied over the entire rotation profile and in conjunction with the ideal stability criterion. Rotation damping and global rotation collapse observed in plasmas exceeding $\beta_{Nno\text{-}wall}$ contrasts the damping observed during tearing mode activity and can be described by drag due to neoclassical toroidal viscosity (NTV) in the helically perturbed field of an ideal displacement. Resonant field amplification of an applied n = 1 field perturbation has been measured and increases with increasing β_N. Equilibria are reconstructed including measured ion and electron pressure, toroidal rotation, and flux iso-surface constraint in plasmas with core rotation ω_ϕ/ω_A up to 0.48. Peak pressure shifts of 11% of the minor radius from the magnetic axis have been reconstructed.

1. Introduction

Stabilizing modes that limit plasma beta is a key goal in fusion reactor design. The National Spherical Torus Experiment, NSTX, [1] has demonstrated the advantages of low aspect ratio geometry in accessing high $\beta_t \equiv 2\mu_0\langle p\rangle/B_0^2$ and $\beta_N \equiv 10^8\langle\beta_t\rangle aB_0/I_p$, where p is the plasma pressure, B_0 is the vacuum toroidal field at the plasma geometric center, and I_p is the plasma current. Plasmas have reached β_t = 39% through boundary and profile optimization [2] and β_N = 6.8 utilizing moderate current profile modification. ST devices normally achieve higher β_N than devices with higher aspect ratio and the present result represents the highest β_N yet achieved in the ST. High $\beta_N \geq 6$ plasmas exceed the ideal no-wall magnetohydrodynamic (MHD) limit, $\beta_{Nno\text{-}wall}$, computed by the DCON code [3] and can remain passively stabilized with $\beta_N/\beta_{Nno\text{-}wall} > 1.3$ for periods greatly exceeding the wall eddy current decay time, τ_w.[4] Toroidal rotation collapse typically correlates with reduction from peak β_N. Understanding the unstable mode spectrum, the physics of instability-induced rotation damping, critical rotation frequency for mode stabilization, and active feedback control has general application to toroidal magnetic confinement systems including ITER.

2. Beta-limiting Instabilities

Global MHD instabilities are observed to limit beta in NSTX plasmas. The ideal MHD kink/ballooning mode can be stabilized by passive conducting wall structure and finite plasma rotation.[5-7] However below a critical rotation frequency, Ω_{crit}, the resistive wall mode (RWM), a kink mode modified by the presence of a conducting wall, can become unstable and grow, leading to rapid rotation damping and beta collapse on the wall eddy current decay time.[8-10] The RWM has a growth rate and real frequency ~ $O(1/\tau_w)$ ~ 100 Hz. Large scale resistive plasma tearing modes also limit beta and reduce plasma rotation but on a timescale typically longer than τ_w.[11] These modes can have growth rates similar to the RWM but have measured frequencies nearly equal to the plasma rotation frequency, ω_ϕ, in the region of the island. Typically $\omega_\phi/2\pi$ ~ 10 kHz in neutral beam heated plasmas. The ideal kink/RWM perturbation can also trigger pure toroidal mode number n = 1 - 3 tearing modes. [4]

The present work focuses on wall stabilization physics of kink/RWM instabilities in high beta ST plasmas. Extensive research has been conducted on the RWM and the mode has been successfully stabilized for times significantly exceeding both τ_w and the energy confinement time, τ_E.[4,12-13] Study has focused on the RWM with n = 1 since it is typically the least stable RWM in tokamaks, minimizing the field line bending of the dominant toroidal field. Theoretical calculations show that high beta spherical torus plasmas, where the vacuum toroidal field is significantly lower, allows n = 2 and higher modes to be unstable at β_N values close to the value at which the n = 1 mode becomes unstable.[4,14] Research of the higher-n instabilities is important to the development of systems to stabilize these modes and sustain operation at the highest plasma beta. The Fitzpatrick-Aydemir (F-A) model [15,16] of the resistive wall mode is used throughout this work to compare experimental observations to theory. This theory has been used to successfully model timescales of RWM response to error field alteration in HBT-EP. [17]

3. Mode Spectrum and Dynamics

NSTX has a major radius, R = 0.86m, aspect ratio, $A \geq 1.27$, plasma current I_p up to 1.5 MA, and $B_0 < 0.6$T. A recently installed array of magnetic field sensors allows the measurement of low frequency n = 1 – 3 modes. The device is equipped with 48 toroidally segmented passive copper stabilizer plates, covered with carbon tiles as plasma facing components. These segments are arranged symmetrically in four toroidal rings, two above and two below the device midplane. The plates are independently connected to the stainless steel vacuum vessel by high resistance supports. Magnetic loops measuring the radial, B_r, and poloidal, B_p, flux are located at each of the plates closest to the midplane; the B_r sensors mounted between the carbon tiles and the copper shells and the B_p sensors mounted a few centimeters below each plate. The sensors are instrumented to detect frequencies up to 2.5 kHz.

Unstable RWMs with n = 1-3 have been observed in high beta NSTX plasmas. The mode spectrum and dynamics for discharges showing pure mode growth, and mode rotation during growth are shown in FIG. 1. Mode growth and associated beta collapse occur in a few τ_w (about 5 ms). The B_p sensor array shows nearly simultaneous growth of n = 1-3 modes in FIG. 1a at a peak β_t = 35% and the measured toroidal phases (n = 1 phase, ϕ_{Bp}, is shown) do not show mode rotation. RWM dynamics from F-A theory indicates that the mode may rotate as the plasma becomes unstable. This is observed in the plasma shown in FIG. 1b. As expected by theory, the measured mode rotation frequency of 120 Hz is ~ $O(1/\tau_w)$ and the mode phase propagation is in the direction of plasma rotation. At this rate, the mode significantly slips behind the measured edge plasma rotation frequency of 2 kHz. The phase

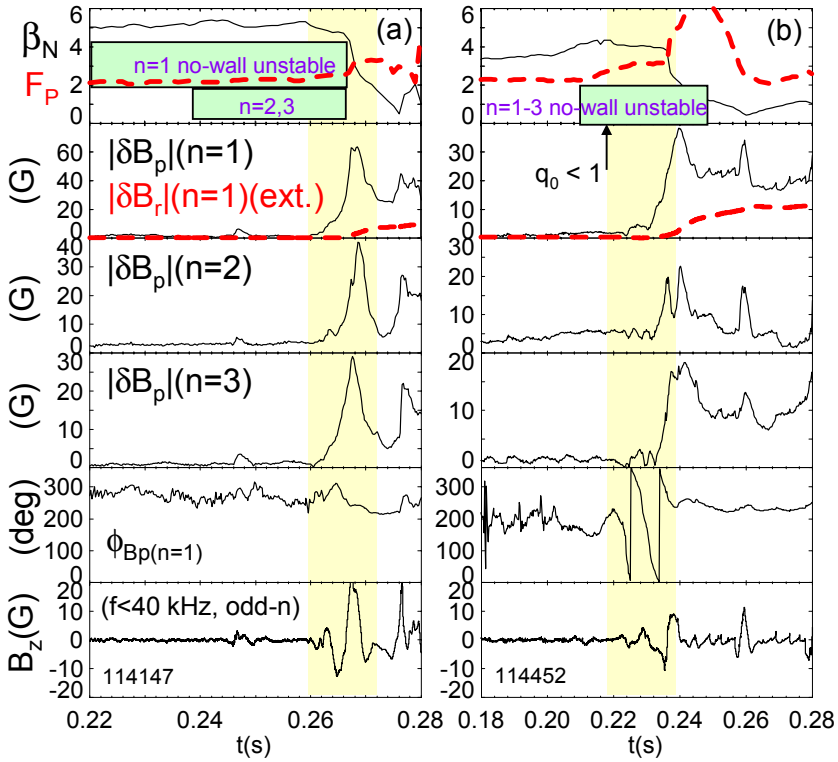

FIG. 1. RWM toroidal mode spectrum and dynamics for pure growth (a) and mode rotation during growth (b).

velocity changes in time as the mode rotates through the toroidal location of maximum error field. The $n = 1$ locked mode detector external to the vacuum vessel begins to measure the RWM about τ_w after it is observed on the B_p sensors due to mode penetration of the vessel, measures a factor of five less signal, and is not capable of detecting the detailed phase shift during RWM growth. Odd-n tearing modes with frequency less than 40 kHz are absent. A rapidly rotating (20 kHz) n=2 mode exists throughout the high beta phase, which is easily distinguished from the RWM.

Time-evolved ideal MHD stability assuming no stabilizing wall for n= 1-3 modes was computed for these plasmas with DCON using time-evolved EFIT [7, 18] equilibrium reconstructions. FIG. 1(a,b) shows that before RWM mode growth, both plasmas exceed the computed n = 1-3 ideal no-wall beta limit. Equilibrium variations were considered for the stability calculations by varying the minimum q between 1.1 – 1.7 and n = 1-3 modes remained unstable for equilibria approaching the time of RWM growth. Visible light emission from the plasma shown in FIG. 1a is compared to the DCON computed perturbed magnetic field normal to the surface in FIG. 2. The computation uses an EFIT experimental equilibrium reconstruction and the illustration includes the sum of the n = 1-3 components scaled to the

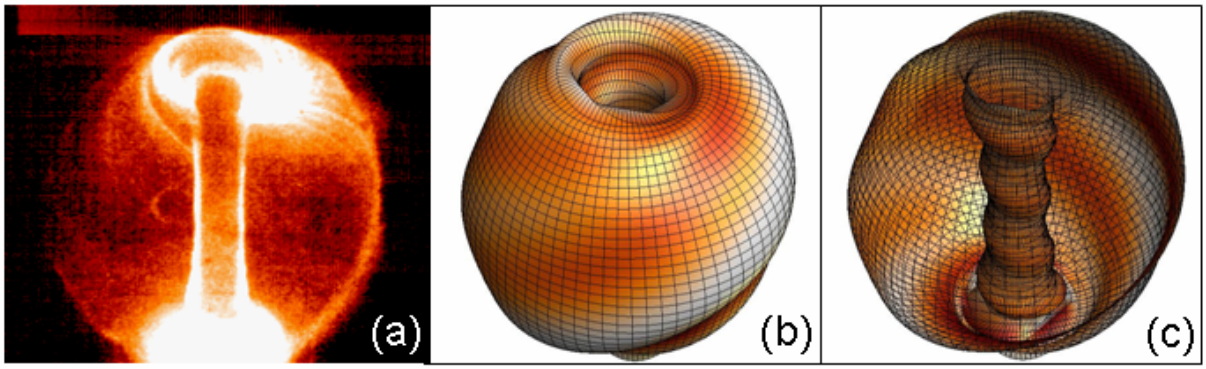

FIG. 2. Visible light emission (a) and DCON computed normal perturbed field (b,c) for the unstable RWM shown in FIG. 1a. (discharge 114147) at t = 0.268s.

measured RWM sensor amplitudes and relative phases. The perturbed field amplitude shown has been scaled up by a factor of 10 to clarify the mode shape. Based on the measured field amplitudes for n = 1-3, an estimate of the real space displacement of the mode is about 3 cm

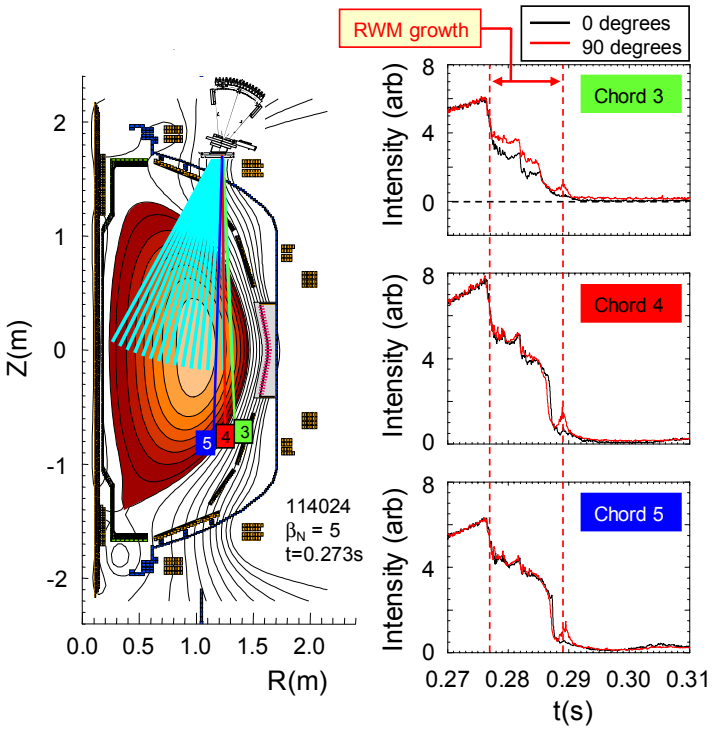

FIG. 3. Toroidal asymmetry of measured soft X-ray emission during RWM growth.

at large major radius. Fast camera images confirm the toroidal asymmetry and macroscopic scale of the mode.

Soft X-ray emission (SXR) measured at two toroidal positions 90 degrees apart shows that the RWM is not localized to a narrow edge region, as assumed by F-A theory. FIG. 3 shows the measured toroidal non-axisymmetry of the SXR during RWM growth. In this particular plasma, the mode is not apparent in the core of the plasma (R = 1.18m, normalized poloidal flux $\psi_n \sim 0.13$) but appears in the channel at $R = 1.31$m ($\psi_n \sim 0.4$). The change in electron temperature, T_e, measured by the midplane Thomson scattering diagnostic for similar RWM plasmas shows the perturbation to be maximum at about 1.3m and greatly reduced in the plasma core.

4. Wall Stabilization Physics

Sustaining $\beta_N > \beta_{Nno\text{-}wall}$ for periods significantly longer than the RWM growth time requires mode stabilization. Plasma rotation frequencies normalized to the Alfven frequency, ω_ϕ/ω_A, of a few percent relative to the mode can passively stabilize the RWM in theory and experiment. This ratio is typically measured at the dominant rational surface (e.g. $q = 2$ in DIII-D). Previous NSTX research reported a possible decrease of Ω_{crit} with increasing q. [4] Considering Ω_{crit} as a profile, rather than a scalar, plasmas operating at high $\beta_N > \beta_{Nno\text{-}wall}$ for long-pulses in NSTX [19] have toroidal rotation frequency profiles greater than $\Omega_{crit}(q)$. The critical rotation frequency of Bondeson and Chu, [20] $\Omega_{crit} = \omega_A/(Cq^2)$ with $C = 4$ well describes RWM stability in conjunction with the ideal stability criterion when applied over the entire rotation profile. This is shown in FIG. 4, where ω_ϕ/ω_A is plotted vs. q at each radial position and time when ω_ϕ is measured for two classes of discharges analyzed for ideal $n = 1$ stability with DCON using time-evolved EFIT equilibrium reconstructions. In the discharges described by triangles, ω_ϕ/ω_A never greatly exceeds $1/(4q^2)$. These plasmas do not sustain $\beta_N > \beta_{Nno\text{-}wall}$ for longer than a few τ_w (e.g. discharge 107636 in Ref [4]) without suffering a beta collapse that restores ideal stability. In contrast, plasmas described by plusses maintain $\beta_N > \beta_{Nno\text{-}wall}$ (about 4.8 in these plasmas) at each time point shown - significantly longer than a few τ_w. In these plasmas, the ω_ϕ/ω_A profile always exceeds $1/4q^2$. Plasma rotation and dissipation from ion Landau damping have been linked to RWM stabilization. However, drift-kinetic theory indicates that trapped particle effects strongly reduce ion Landau damping and increase the Pfirsch-Schluter toroidal inertia enhancement in the RWM range of frequencies.[20] The relative importance of inertia over dissipation is consistent with the observed RWM stabilization at increased q in NSTX. Note that high β_N plasmas can be stabilized with a

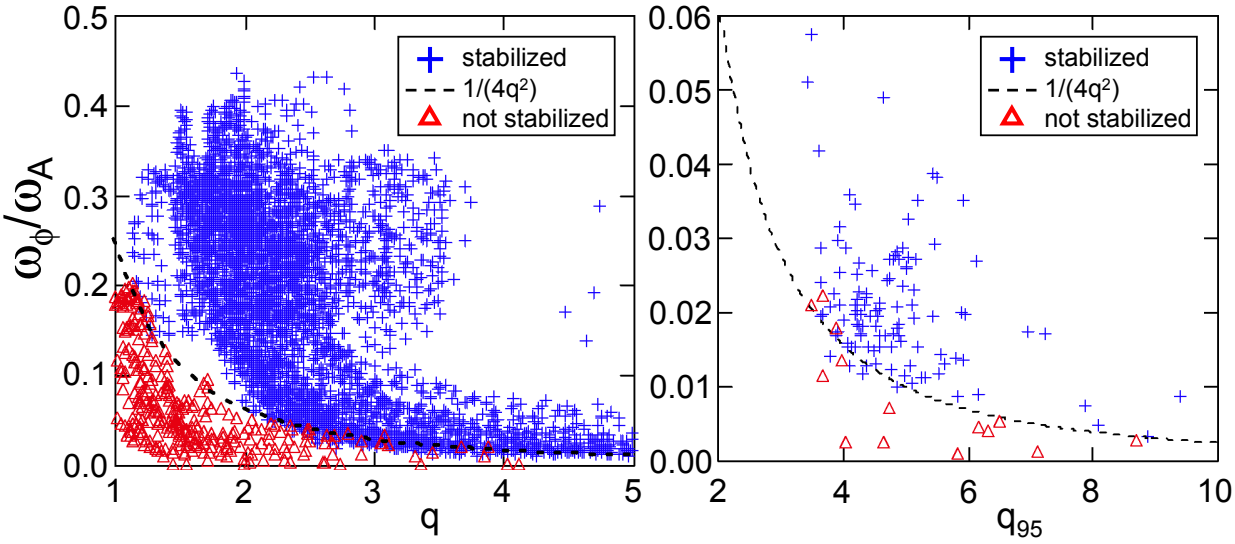

FIG. 4. Observed kink/RWM stability vs. local ω_ϕ/ω_A, parameterized by local q value (frame (a)) and q_{95} (frame (b)). Ω_{crit} is well defined by the Bondeson-Chu expression $\omega_A/(4q^2)$.

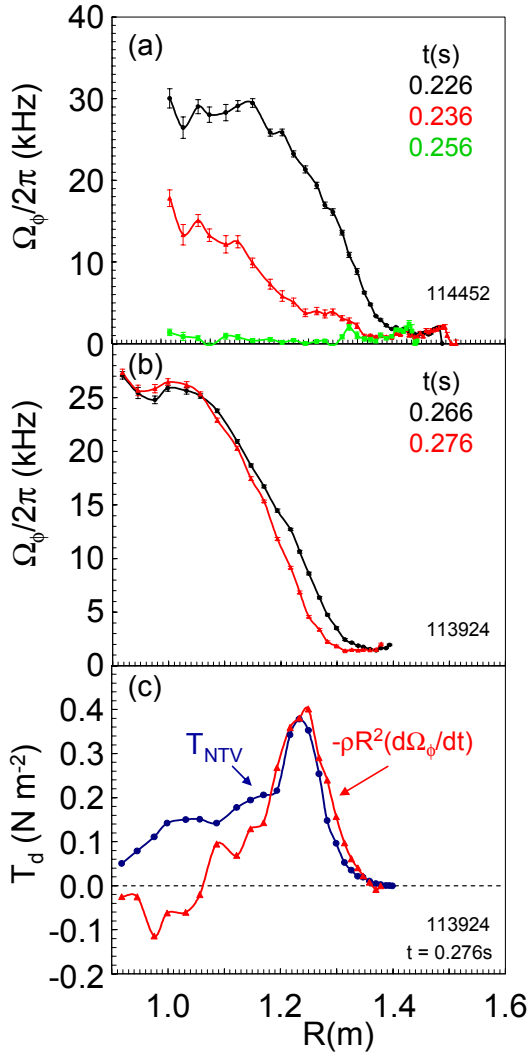

FIG. 5. Rotation damping during RWM (a,b) NTV damping torque vs. measurement (c).

portion of the ω_ϕ/ω_A profile dropped below $1/4q^2$, but beta collapses can result if this occurs at low-order rational surfaces.

Standard F-A theory yields a scaling of $\Omega_{crit} \sim 1/q$, rather than $1/q^2$ as shown in the work of Bondeson-Chu. The former does not match NSTX data as well as the latter. One might expect that the difference could be due to the localization of the inertial layer for RWM dynamics to the plasma edge in the F-A theory which is computed to be about the outer 10% of the poloidal flux for NSTX. However, if we examine $\Omega_{crit}(q = q_{95})$, within the F-A inertial layer, measurements still support the Bondeson-Chu scaling (FIG. 4b). The F-A model reproduces this scaling if neoclassical viscosity is used. [21] The application of neoclassical viscosity yields the toroidal inertia enhancement, lowering the effective Alfven frequency and reducing Ω_{crit} by an additional factor of $1/q$ compared to the standard F-A result using classical perpendicular inertia.

Rotation damping in plasmas below $\beta_{No\text{-}wall}$ can be described by electromagnetic drag due to small magnetic islands and associated viscous plasma coupling. [22] Large-scale MHD modes, especially the 1/1 internal mode and the RWM in NSTX, can cause rapid rotation damping. Understanding the rotation damping physics of these modes is important to sustaining passive stabilization. The large rotation damping

enhancement and global rotation collapse observed during RWM growth (FIG. 5a,b) can be described by non-resonant drag due to neoclassical toroidal viscosity (NTV) in the helically perturbed field of the mode. [23] By associating the magnitude of the perturbed field to the measured δT_e, NTV calculations show qualitative agreement between theory and experiment (FIG. 5c) during the start of the global rotation collapse (FIG. 5b). NTV, which depends on the field perturbation and ion temperature as $\delta B^2 * T_i^{0.5}$ may explain the lack of damping and sustained plasma rotation ~ 2 kHz observed at the plasma edge where T_i is small. Unlike rotation damping due to islands, momentum transfer across a resonant surface is not observed during RWM rotation damping. Low frequency tearing modes were absent during the rotation collapses shown. Details of the rotation damping profile and the role of NTV in rotation damping due to the 1/1 internal mode are examined in Ref. 11.

5. Non-axisymmetric Fields and Resonance Effects

Two coils, of an eventual six to be used for active stabilization of the RWM have been used to study resonant field amplification (RFA) [24,25] and to slow rotation below Ω_{crit} by generating n = 1 standing wave error field perturbations. The coils are external, but closely fitted to the vacuum vessel, are diametrically opposed, and each cover about 60 degrees of toroidal angle. The coils were designed using VALEN [26] and are located between the upper and lower primary passive stabilizing plates to minimize coil-to-plate coupling. [4]

Pre-programmed square wave (DC) and low frequency (20 – 60 Hz) n=1 magnetic field pulses were applied to the plasma clearly generating RFA and at sufficiently large field amplitude caused RWM destabilization. RFA generally increases with β_N, similar to results in DIII-D. [25] The measured RFA gain, defined as in Ref [25], is measured to be in the same range (0 – 3.5 G/kA-turn) reported on DIII-D at lower β_N (FIG. 6). While n > 1 unstable RWMs have been generated, the RFA generated from the applied n = 1 field and measured during periods of RWM stability is also observed to have n = 1.

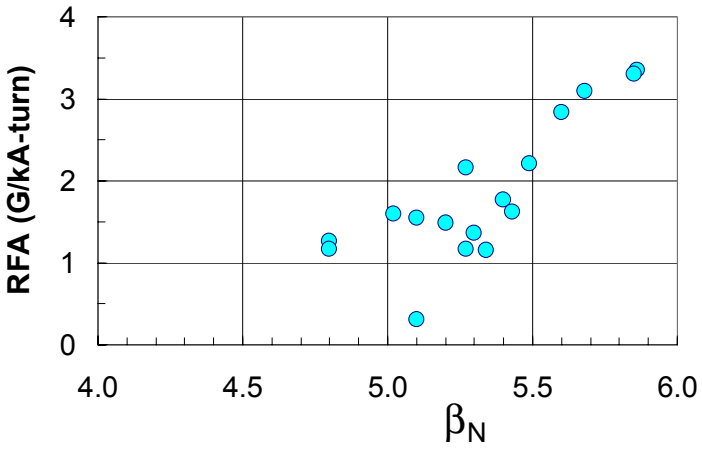

FIG. 6. n=1 resonant field amplification vs. β_N for an externally applied n=1 magnetic field.

A strong correlation between the frequency of AC components of the equilibrium field and the RWM in high beta, low q plasmas has been observed. This correlation is possibly due to interaction of the mode with AC error fields from the equilibrium coil systems or stabilizing plate eddy currents. The phenomena also matches the dynamics theoretically explained by the F-A model of the mode matching frequency with the AC error field as the mode goes unstable. The effect is shown in FIG. 7 with β_t decreasing from a maximum of 34% during 15 kHz, n=1 tearing mode activity. The toroidal rotation is below the critical profile for RWM stabilization $\omega_\phi/\omega_A(q) < 1/(4q^2)$ over the entire pulse duration. As the mode rotates and grows, it matches frequency at 385 Hz with the power supply ripple observed on several shaping coils (PF2 coil current is shown). The dynamics of the measured amplitude and phase closely resemble the F-A model results published in Ref. [16], figs. 8 and 10. Initially, the n=1 mode phase oscillates about some angle and eventually begins to rotate. The rotating mode phase velocity is not constant, also in agreement with the theory (Ref. [16],

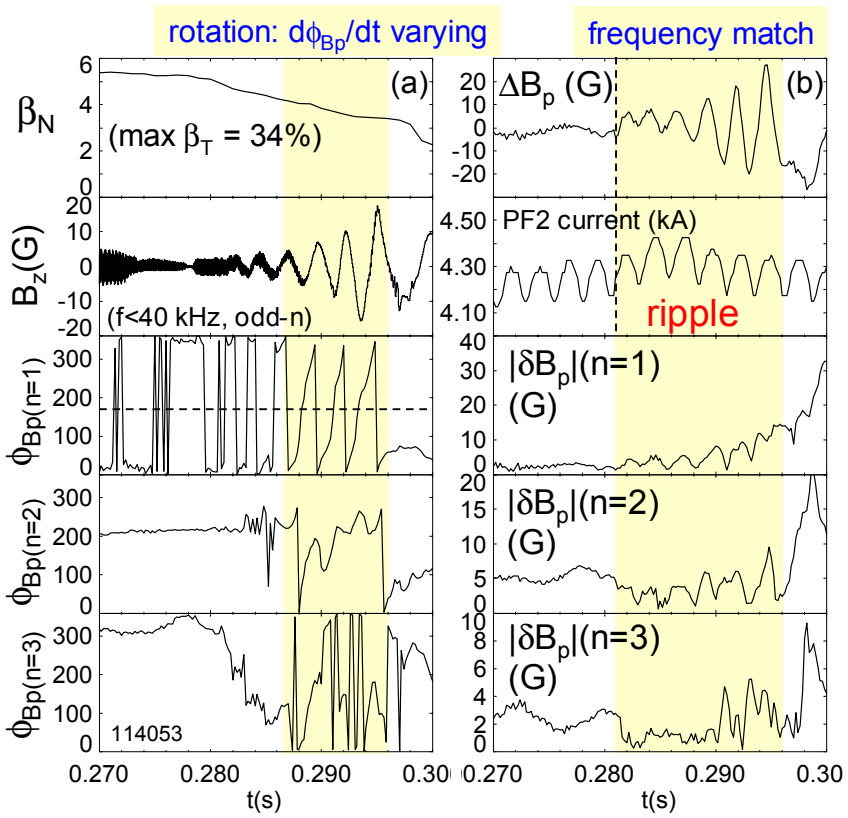

FIG. 7. RWM sensor array phase and amplitude for mode with apparent phase lock / resonance at 385 Hz.

fig. 10 frames (3,4)). Similar to the RWM in FIG. 1b, the phase velocity changes as the mode phase approaches then traverses the toroidal position of maximum intrinsic error field. However, in this case, the mode phase propagation is *counter* to the direction of plasma rotation. This can occur for the "kink mode branch" of the F-A dispersion relation [15]. The n=1-3 modes have similar peak amplitudes during the rotating period, but n=2,3 have different dynamics than the n = 1 mode. Comparison of the difference between two opposing B_p sensors, ΔB_p, and the decomposed n=1-3 mode amplitudes shows that the n=2,3 modes comprise a significant fraction of the total signal. Because of this, the local maxima of the n=1 amplitude appear flattened compared to ΔB_p. The n= 3 mode has the largest amplitude near the n=1 peak amplitude, but the n=2 mode does not always follow this relationship. Rotating n=1,2 modes (15 and 30 kHz respectively) are measured by magnetic pickup coils but are distinguishable from the RWMs by their greatly disparate frequencies.

6. Plasma Rotation and Equilibrium Reconstruction

The importance of rotation in altering the high beta equilibrium has become apparent in discharges heated by intense co-injected neutral beams. Maximum core toroidal rotation frequencies $\omega_\phi/\omega_A = 0.48$ have been measured. NSTX EFIT reconstructions can now include measured ion pressure and toroidal rotation, V_ϕ, profiles (FIG. 8). The full solution to the Bernoulli equation is used. Topological flux surface constraints [27] are also imposed using the measured $T_e(R)$ to maintain consistency of the equations solved. Reconstruction quality is improved by the expanded physics model and flux iso-surface (isotherm) constraints. Discharges with high V_ϕ (FIG. 8a) exhibit a clear outward shift of total pressure (white contours) from magnetic flux surfaces (black contours) in the plasma core. Peak shifts of 11% have been reconstructed. The fitted plasma dynamic pressure $P_d = 1/2\rho V_\phi^2$, where ρ is the plasma mass density, is typically more peaked than the total pressure, P_t (FIG. 8c,b). The reconstructed q_0 decreases in time compared to static reconstructions with high $q_0 > 2.5$. These results provide initial insight on the potential alteration of plasma stability and Ω_{crit} calculations. The reconstructions offer input for future computation of stability with rotation. While the variation of local equilibrium quantities is evident in rotating plasmas, the global

stored energy remains generally unchanged from that of static reconstructions. Analysis of a few thousand shot-times shows a variation between static and rotating models of about 3%.

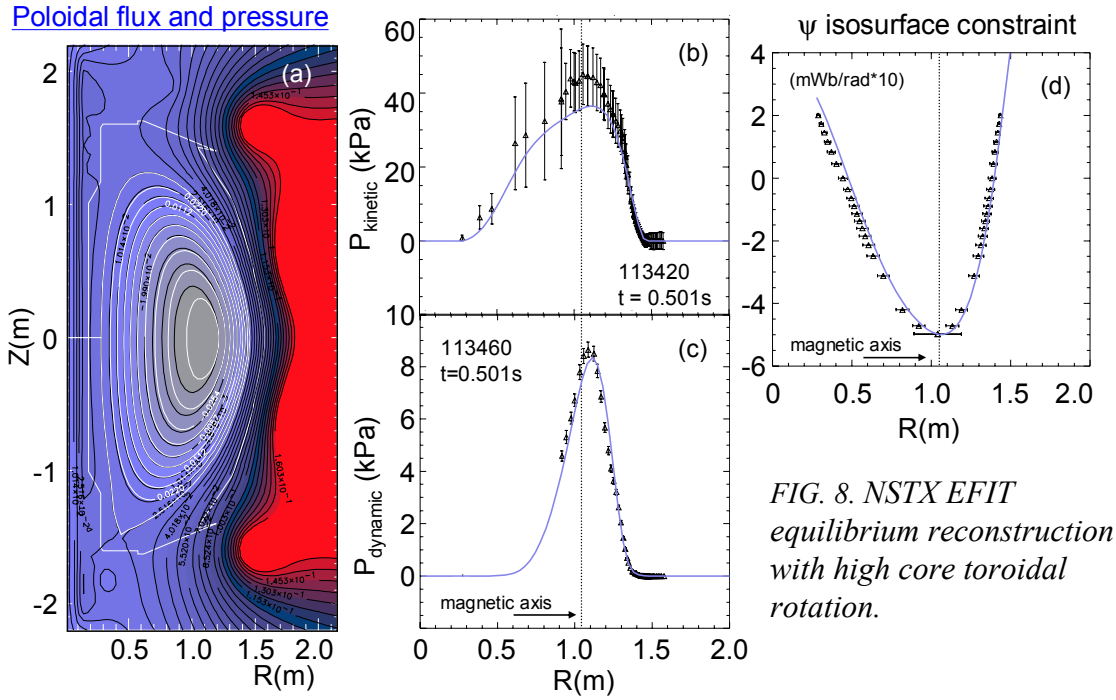

FIG. 8. NSTX EFIT equilibrium reconstruction with high core toroidal rotation.

[1] ONO, M., KAYE, S.M., PENG, Y.-K.M., et al. Nucl. Fusion **40** (2000) 557.
[2] KAYE, S.M., BELL, M.G., BELL, R.E., et al., this conference, Paper OV/2-3.
[3] GLASSER, A.H. and CHANCE, M.C., Bull. Am. Phys. Soc. **42** (1997) 1848.
[4] SABBAGH, S.A., BIALEK, J.M., BELL, R.E., et al., Nucl. Fusion **44** (2004) 560.
[5] CALLEN, J.D., et al., Phys. Plasmas **6** (1999) 2963.
[6] GAROFALO, A.M., STRAIT, E.J., et al., Phys. Rev. Lett. **89** (2002) 235001-1.
[7] SABBAGH, S.A., KAYE, S.M., MENARD, J.E., et al., Nucl. Fusion **41** (2001) 1601.
[8] BONDESON, A., and WARD, D.J., Phys. Rev. Lett. **72** (1994) 2709.
[9] GAROFALO, A.M., TURNBULL, A.D., et al., Phys. Rev. Lett. **82** (1999) 3811.
[10] SABBAGH, S.A., BELL, R.E., BELL, M.G., et al., Phys. Plasmas **9** (2002) 2085.
[11] MENARD, J.M., BELL, R.E., GATES, D.A., this conference, Paper EX/P2-26.
[12] GAROFALO, A.M., JENSEN, T.H., et al., Phys. Plasmas **9** (2002) 1997.
[13] OKABAYASHI, M., BIALEK, J.M., et al., Phys. Plasmas **8** (2001) 2071.
[14] MENARD, J.E., JARDIN, S.C., KAYE, S.M., et al., Nucl. Fusion **37** (1997) 595.
[15] FITZPATRICK, R., AYDEMIR, A., Nucl. Fusion **36** (1996) 11.
[16] FITZPATRICK, R., Phys. Plasmas **9** (2002) 3459.
[17] SHILOV, M., CATES, C., JAMES, R., et al., Phys. Plasmas **11** (2004) 2573.
[18] LAO, L.L., et al., Nucl. Fusion **25** (1985) 1611.
[19] MENARD, J.E., BELL, M.G. BELL, R.E., et al., Nucl. Fusion **43** (2003) 330.
[20] BONDESON, A., CHU, M.S., Phys. Plasmas **3** (1996) 3013.
[21] SHAING, K.C., "Neoclassical dissipation and resistive wall modes in tokamaks", to be published in Phys. Plasmas.
[22] FITZPATRICK, R., Nucl. Fusion **33** (1993) 1049.
[23] SHAING, K.C., HIRSHMAN, S.P., and CALLEN, J.D., Phys. Fluids **29** (1986) 521.
[24] BOOZER, A.H., Phys. Rev. Lett. **86** (2001) 5059.
[25] GAROFALO, A.M., JENSEN, T.H., and STRAIT, E.J. **10** (2003) 4776.
[26] BIALEK, J.M, BOOZER, A.H., MAUEL, M.E., et al., Phys. Plasmas **8** (2001) 2170.
[27] ZHANG, C., LAO, L.L., "Tokamak Equilibrium Reconstruction with Topological and Current Hole Constraints", General Atomics Report A24582.